Zornberg, J.G. (2011). "Advances in the Use of Geosynthetic for Waste Containment." Invited Keynote Paper, Proceedings of the *Fifteenth African Regional Conference on Soil Mechanics and Geotechnical Engineering*, Maputo, Mozambique, July 17-21, pp. 1-21 (CD-ROM).

Advances in the Use of Geosynthetics for Waste Containment

Jorge G. Zornberg, Ph.D., P.E.
The University of Texas at Austin, USA
President, International Geosynthetics Society (IGS)

Abstract

Waste containment facilities are among the geotechnical systems that make use of most of the geosynthetic types in all identified functions (e.g. reinforcement, drainage, filtration). The inclusion of geosynthetic components is likely to expand as manufacturers develop new and improved materials and as engineers/designers develop analysis routines for new applications. This paper focuses on specific advances involving the use of geosynthetics in the different components of waste containment facilities. In particular, this paper addresses recent advances on the stability of landfill liners involving GCLs, design of liquid collection layers, reinforced cover systems, and exposed geomembrane covers. Recent case histories are also provided to document the implementation of these advances in engineering practice.

Resumo

Instalações de disposição final de resíduos são, entre todos os sistemas geotécnicos, os que empregam a maior diversidade de geosintéticos com distintas funções (e.g. reforço, drenagem, filtragem). O uso de componentes geosintéticos tende a expandir-se com o contínuo desenvolvimento e melhora de novos materiais, e com o desenvolvimento, por parte de engenheiros e projetistas, de novos procedimentos de análise visando novas aplicações. O presente trabalho tem por objetivo descrever vantagens específicas envolvendo o uso de geosintéticos nos diferentes componentes de sistemas de contenção de resíduos. Em particular, o trabalho aborda recentes aspectos relativos à estabilidade de barreiras em aterros sanitários envolvendo GCLs, projeto de camadas para coleta de líquidos, sistemas reforçados de coberturas, e sistema de cobertura composto por geomembranas expostas. Exemplifica-se o emprego dos avanços técnicos descritos com casos históricos recentes.

1 INTRODUCTION

Geosynthetics play an important role in environmental applications because of their versatility, cost-effectiveness, ease of installation, and good characterization of their mechanical and hydraulic properties. Geosynthetics also can offer a technical advantage in relation to traditional liner systems or other containment systems. The use of geomembranes as the primary water proofing element at the Contrada Sabetta Dam, Italy (Cazzuffi 1987) and to keep an upstream clay seepage control liner from dessicating in the Mission Dam (today Terzaghi Dam), Canada (Terzaghi & Lacroix 1964) in the late 1950's represent applications that have been the precursors of today's usage of geosynthetics in containment systems. Both applications predated the use of conventional geosynthetics by some 20 years. Geosynthetics systems are nowadays an accepted and well-established component of the landfill industry (since at least early 1980's). Containment systems for landfills typically include both geosynthetics and earthen material components, (e.g. compacted clays for liners, granular media for drainage layers, and various soils for protective and vegetative layers).

The state of the art on the use of geosynthetics in waste containment facilities previous to this period has been documented by various important sources, which have set the path for the growth of geosynthetics in this field (e.g. Giroud & Cazzuffi 1989; Koerner 1990; Cancelli & Cazzuffi 1994;

Gourc 1994; Rowe et al. 1995; Manassero et al. 1998; Rowe 1998; Bouazza et al. 2002).

Focus of this paper is on stability of liners involving GCLs, geosynthetics in liquid collection systems, reinforced cover systems, and exposed geomembrane covers. Recent case histories are also provided to document the implementation of recent advances in engineering practice.

2 GEOSYNTHETICS IN LANDFILLS

The multiple uses of geosynthetics in the design of modern municipal solid waste landfills is a good illustration of an application in which the different geosynthetics can be and have been used to perform all the functions discussed previously. Virtually all the different types of geosynthetics discussed previously have been used in the design of both base and cover liner systems of landfill facilities. Fig. 1 illustrates the extensive multiple uses of geosynthetics in both the cover and the base liner systems of a modern landfill facility (Zornberg & Christopher 2007). The base liner system illustrated in Fig. 1 is a double composite liner system. Double composite liner systems are used in some instances for containment of municipal solid waste and are frequently used for landfills designed to contain hazardous waste. The base liner system shown in the figure includes a geomembrane/GCL composite as the primary liner system and a geomembrane/compacted clay liner composite as the secondary system. The leak detection system, located between the primary and secondary liners, is a geotextile/geonet composite. The leachate collection system overlying the primary liner on the bottom of the liner system consists of gravel with a network of perforated pipes. A geotextile protection layer beneath the gravel provides a cushion to protect the primary geomembrane from puncture by stones in the overlying gravel. The leachate collection system overlying the primary liner on the side slopes of the liner system is a geocomposite sheet drain (geotextile/geonet composite) merging into the gravel on the base. A geotextile filter covers the entire footprint of the landfill and prevents clogging of the leachate collection and removal system. The groundwater level may be controlled at the bottom of the landfill by gradient control drains built using geotextile filters. Moreover, the foundation soil below the bottom of the landfill may be stabilized as shown in the figure using randomly distributed fiber reinforcements, while the steep side soil slopes beneath the liner could also be reinforced using geogrids. Different types of geosynthetics (e.g. geogrids, geotextiles, fibers) could have been selected for stabilization of the foundation soils.

The cover system of the landfill illustrated in Fig. 1 contains a composite geomembrane/GCL barrier layer. The drainage layer overlying the geomembrane is a geocomposite sheet drain (composite geotextile/geonet). In addition, the soil

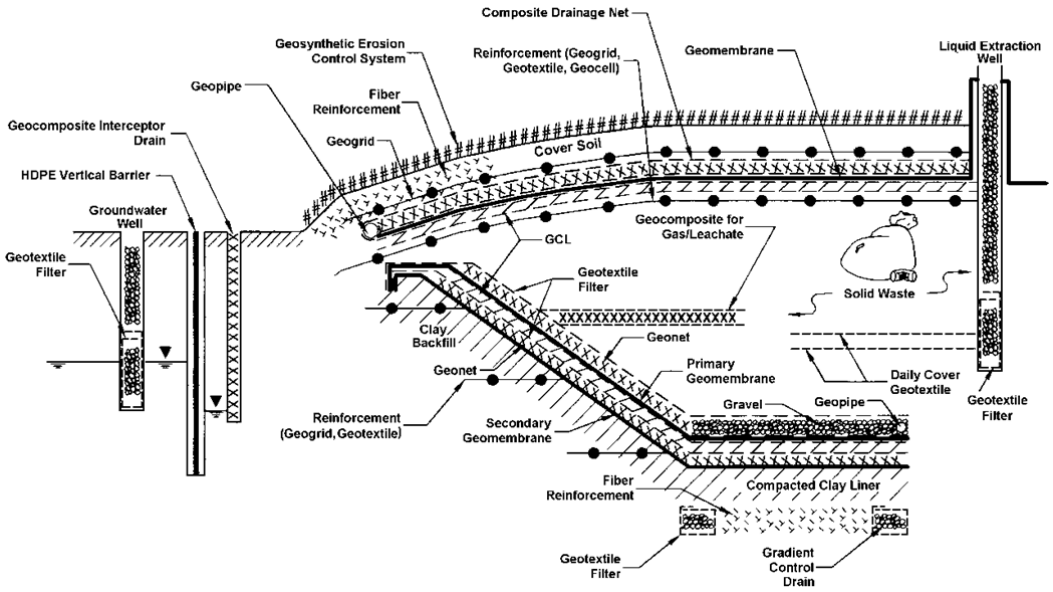

Figure 1. Multiple uses of geosynthetics in landfill design (from Zornberg & Christopher 2007).

cover system may include geogrid, geotextile, or geocell reinforcements below the infiltration barrier system. This layer of reinforcements may be used to minimize the strains that could be induced in the barrier layers by differential settlements of the refuse or by a future vertical expansion of the landfill. In addition, the cover system could include a geogrid or geotextile reinforcement above the infiltration barrier to provide stability to the vegetative cover soil. Fiber reinforcement may also be used for stabilization of the steep portion of the vegetative cover soil. A geocomposite erosion control system above the vegetative cover soil is indicated in the figure and provides protection against sheet and gully erosion. Fig. 1 also illustrates the use of geosynthetics within the waste mass, which are used to facilitate waste placement during landfilling. Specifically, the figure illustrates the use of geotextiles as daily cover layers and of geocomposites within the waste mass for collection of gas and leachate. Geosynthetics can also be used as part of the groundwater and leachate collection well system. The use of geotextiles as filters in groundwater and leachate extraction wells is illustrated in the figure. Finally, the figure shows the use of an HDPE vertical barrier system and a geocomposite interceptor drain along the perimeter of the facility. Although not all of the components shown in Fig. 1 would normally be needed at any one landfill facility, the figure illustrates the many geosynthetic applications that can be considered in landfill design.

3 STABILITY OF LINERS INVOLVING GCLS

The primary design concern when GCLs are placed in contact with other geosynthetics or soils on a slope is the interface shear strength, which must be sufficiently high to transmit shear stresses that may be generated during the lifetime of the facility. Another concern is the possible internal failure of the GCL (within the bentonite or at the interface between the bentonite and its carrier geosynthetics). The need for a more careful design of lining systems has been stressed by the recent failures generated by slip surfaces along liner interfaces (Byrne et al. 1992; Stark et al. 1998). Much effort has been devoted in the past decade to improve the understanding of the different factors affecting the shear resistance of the different interfaces present in liner systems.

A comprehensive review concerning GCL internal and interface shear strength testing, as well as an analysis of a large database of direct shear tests on internal and interface GCL shear strength has been recently completed (McCartney et al. 2002). This study compares the shear strength of interfaces involving different GCL and geomembrane types, focusing on the effects of different conditioning and testing procedures on GCL shear strength (i.e. hydration, consolidation, rate of shearing, normal stress during different stages of testing). Fig. 2a shows a set of 320 test results for the internal shear strength of different reinforced and unreinforced

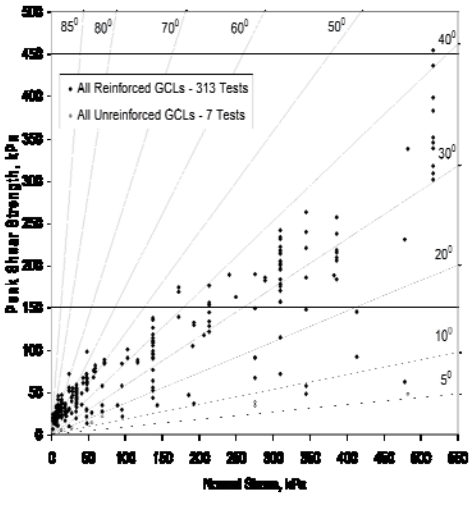

(a)

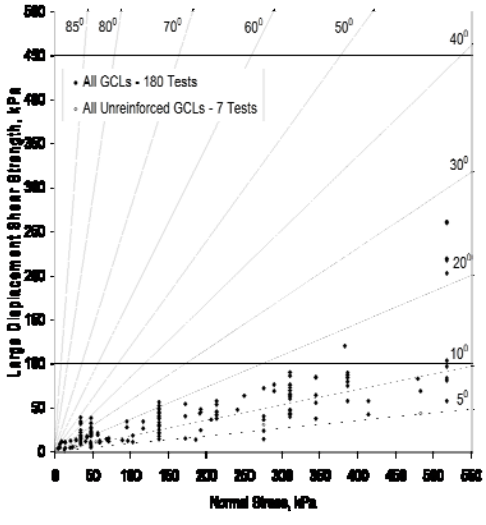

(b)

Figure 2. Reinforced and unreinforced GCLs, (a) Peak shear strength (b) Large-displacement shear strength (McCartney et al. 2002)

GCLs tested under a wide range of conditioning procedures but similar test procedures. All tests were conducted by a single laboratory with test procedures consistent with ASTM D6243. Similarly, Fig. 2b shows the large-displacement (50-75 mm) shear strength of 187 of the GCLs referred to in Fig. 2a. There is significantly less variation in the large displacement shear strength, although the shear strength is still slightly greater than the residual shear strength of unreinforced sodium bentonite. Similar trends in peak and large displacement shear strengths were observed in this study for the GCL-geomembrane interfaces. The variation in shear strength for varying GCL type and conditioning procedures emphasize the importance of conducting site and product specific laboratory testing for internal and interface GCL shear strength.

McCartney et al. (2002) propose that the conditioning and testing procedures affect the swelling behavior of the GCL, resulting in variable material properties and either positive or negative excess pore water pressures generated during shearing. Variability associated with the swelling of the GCL is ultimately related to the variability in the internal or interface shear strength. These results are generally consistent with laboratory results conducted in several other studies (Stark & Eid 1996, Gilbert et al. 1996, Eid & Stark 1997, Fox et al. 1998a) on the internal strength of unreinforced and reinforced (stitch bonded and needle punched) GCLs. Peak shear strengths for the unreinforced GCL products were found to be similar and comparable to those for sodium bentonite (i.e. very low shear strength), which makes them prone to instability. Because of this, unreinforced GCLs are usually not recommended for slopes steeper than 10H:1V (Frobel 1996; Richardson 1997). On the other hand, reinforced GCLs have higher internal peak strength due to the presence of fiber reinforcements. The behavior of reinforced GCLs has been shown to depend on the resistance against pullout and/or tensile rupture of the fibers reinforcements and the shear strength of the bentonite (at large displacements once the fibers have failed). The peak shear strength of different types of reinforced GCLs (needle-punched, thermal bonded, stitch-bonded) may differ significantly (McCartney et al. 2002). It is worth noting that despite the fact that internal failure of reinforced GCLs could possibly occur in the laboratory, there are no known cases of slope failures that can be attributed to internal shear failure of reinforced GCLs.

Laboratory interface shear tests are routinely conducted to evaluate interface friction between GCLs and soils or geosynthetics under operating conditions. As a result, a more extensive database is now available (Garcin et al. 1995; Bressi et al. 1995; Feki et al. 1997; Gilbert et al. 1996; Von Maubeuge & Eberle 1998; Eid et al. 1999; Triplett & Fox 2001; McCartney et al. 2002). The major finding worth noting is the possible reduction in frictional resistance between a geomembrane and a GCL due to extrusion of bentonite through woven geotextiles and nonwoven geotextiles with a mass per unit area less than 220 g/m^2 into the adjacent geomembrane interface.

McCartney et al. (2002) observed that different reinforced GCLs would experience different interface shear strengths, implying that sodium bentonite extrusion from the GCL is related to the internal fiber reinforcements in addition to the conditioning procedures.

Despite the observed difference between internal and interface GCL shear strength, variability may still imply that a prescribed approach to laboratory testing may not be acceptable. McCartney et al. (2002) identified that the variability of both internal and interface GCL shear strengths is a key issue in laboratory testing. Interpretation of this variability is necessary to correctly quantify the shear strength of an interface. Fig. 3 shows probability density functions for the peak shear strength of a needle-punched GCL for 19 tests with the same test conditions and procedures. Variability in the internal shear strength is related to the internal fiber reinforcement characteristics as well as changes related to the swelling of the GCL. It is interesting that the interface shear strength has been observed to be only slightly less variable than the internal GCL shear strength. There are several factors that may affect bentonite extrusion from the GCL during hydration, as well as variable frictional connections between textured geomembranes and the woven geotextile of the GCL. It should be noted that variability in the results increases significantly with increasing normal stress.

No full-scale field failures related to the internal shear strength of reinforced GCLs have been reported. This implies that field-testing may be

required to truly determine the critical interface in a layered system. Tanays et al. (1994), Feki et al. (1997) and Daniel et al. (1998) reported the findings from full scale field tests of the internal and interface shear strength behavior of unreinforced and reinforced GCLs configured with other liner components (geomembranes, geotextiles, and soils). Tanays et al. (1994) and Feki et al. (1997) present results on a experimental cell where a stitch bonded GCL was installed on slopes inclined at 2H:1V and 1H:1V respectively. Displacements within the GCL were found to be very low on the 2H:1V slope and remained unchanged during the period of observation (500 days). One day after its installation on the 1H:1V slope, the GCL reached an average strain of 5.5% with extension occurring at the top of the slope. Further displacements decreased with time of observation (3 months). It was assumed that partial failure of the GCL occurred at the measuring points due to excessive strain (> 2%). Significant information concerning interface behavior has been gathered by Daniel et al. (1998). It was reported that all geosynthetic configurations on test slopes inclined at 3H:1V performed satisfactorily. Three slides have occurred on steeper slopes (2H:1V). One slide occurred internally in an unreinforced GCL (a geomembrane backed GCL) because of sodium bentonite hydration. Two slides occurred at the interface between a reinforced GCL and a geomembrane 20 and 50 days after construction. The slides were due to reduction in the interface strength caused by bentonite extrusion through a woven geotextile. Stark et al. (1998) presented a case study describing a slope failure involving an unreinforced GCL in a landfill liner system.

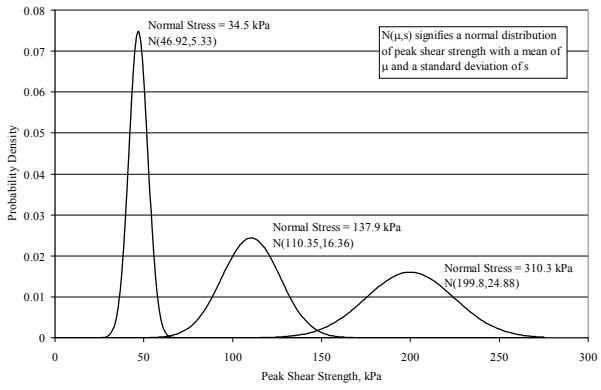

Figure 3. Probability density functions for the internal peak shear strength of a needle-punched GCL, developed from 19 test series of three different normal stresses (McCartney et al. 2002)

4 GEOSYNTHETICS IN LIQUID COLLECTION SYSTEMS

4.1 General considerations

Calculating the thickness of liquid in a liquid collection layer is an important design step because one of the design criteria for a liquid collection layer is that the maximum thickness of the liquid collection layer must be less than an allowable thickness. The term "thickness" is used instead of the more familiar term "depth", because thickness (measured perpendicular to the liquid collection layer slope), and not depth (measured vertically), is actually used in design.

The thickness of liquid in a liquid collection layer depends on the rate of liquid supply. A typical case of liquid supply is that of liquid impinging onto the liquid collection layer. Two examples of liquid collection layers with such a type of liquid supply can be found in landfills (Fig. 4): (i) the drainage layer of the cover system (Fig. 4a), where the liquid that impinges onto the liquid collection layer is the precipitation water that has percolated through the soil layer overlying the drainage layer; and (ii) the leachate collection layer (Fig. 4b), where the liquid that impinges onto the leachate collection layer is the leachate that has percolated through the waste and through the protective soil layer overlying the leachate collection layer. The terminology "liquid impingement rate" is often used in the case of landfills to designate the rate of liquid supply.

Equations are available (Giroud et al. 2000a) to calculate the maximum thickness of liquid in a liquid collection layer that meets the following conditions:

- the liquid supply rate is uniform (i.e. it is the same over the entire area of the liquid collection layer) and is constant (i.e. it is the same during a period of time that is long enough that steady-state flow conditions can be reached);
- the liquid collection layer is underlain by a geomembrane liner without defects and, therefore, liquid losses are negligible;
- the slope of the liquid collection layer is uniform (a situation referred to herein as "single slope") ; and
- there is a drain at the toe of the slope that promptly removes the liquid.

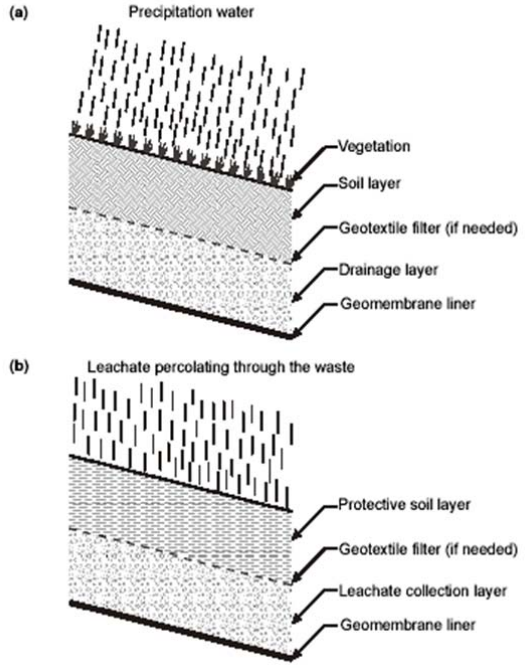

Figure 4. Examples of liquid collection layers subjected to a uniform supply of liquid in a landfill: (a) drainage layer in a cover system; (b) leachate collection layer (Giroud et al. 2000a).

The last two conditions are not met in cases where the liquid collection layer comprises two sections on different slopes, with no drain removing the liquid at the connection between the two sections; in those cases, the only drain is at the toe of the downstream section.

4.2 Shape of the liquid surface and maximum liquid thickness

The shape of the liquid surface in the liquid collection layer in the case where there is a perfect drain at the toe of the liquid collection layer is shown in Fig. 5. The shape of the liquid surface depends on a dimensionless parameter, λ, called "characteristic parameter", and defined as follows:

$$\lambda = \frac{q_h}{k \tan^2\beta} \qquad (1)$$

where: q_h = liquid impingement rate (i.e. rate of liquid supply per unit horizontal area); k = hydraulic conductivity of the liquid collection material in the direction of the flow; and β = slope angle of the liquid collection layer with the horizontal.

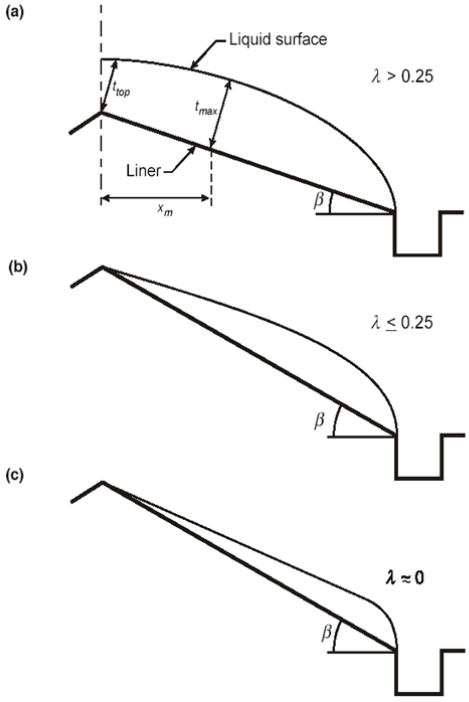

Figure 5. Shape of the liquid surface in a liquid collection layer as a function of the dimensionless characteristic parameter, λ: (a) λ > 0.25; (b) λ ≤ 0.25; (c) λ very small (Giroud et al. 2000a)

The maximum liquid thickness must be estimated for two reasons: (1) the liquid thickness is typically limited by regulations (e.g. the Resource Conservation and Recovery Act in the US limits requires a maximum liquid thickness of 0.3 m), and (2) good design requires that the liquid thickness be less than the thickness of the lateral drain (to avoid confined flow). Regardless of the shape of the liquid surface, the maximum liquid thickness, t_{max} , in the liquid collection layer is given by the following eq., known as the modified Giroud's eq. (Giroud et al. 2000a):

$$t_{max} = j \frac{\sqrt{\tan^2\beta + 4 q_h / k} - \tan\beta}{2\cos\beta} L = j \frac{\sqrt{1+4\lambda}-1}{2} \frac{\tan\beta}{\cos\beta} L \qquad (2)$$

where: L = horizontal projection of the length of the liquid collection layer in the direction of the flow; and j is a dimensionless parameter, called "modifying factor", and defined as follows:

$$j = 1 - 0.12 \exp\left\{-\left[\log(8\lambda/5)^{5/8}\right]^2\right\} \qquad (3)$$

Numerical values of the modifying factor, j, range between 0.88 and 1.00. Therefore, a conservative approximation of Eq. 2 is the following eq., which is known as the original Giroud's eq.:

$$t_{max} = \frac{\sqrt{\tan^2\beta + 4\,q_h / k} - \tan\beta}{2\cos\beta} L = \frac{\sqrt{1+4\lambda}-1}{2} \frac{\tan\beta}{\cos\beta} L \quad (4)$$

An exact solution to the problem was first published by McEnroe (1993). However, this solution is very tedious to use and is subject to significant errors resulting from the number of significant digits used during calculations.

When λ is very small (e.g. $\lambda < 0.01$), which occurs in many practical situations, Eqs. 2 and 4 are equivalent to the following approximate eq. (Giroud et al. 2000a):

$$t_{max} \approx t_{lim} = \frac{q_h}{k \sin\beta} L = \frac{q_h}{k \tan^2\beta} \frac{\tan\beta}{\cos\beta} L = \lambda \frac{\tan\beta}{\cos\beta} L \quad (5)$$

where, t_{lim} is the maximum liquid thickness in the limit case where q_h is small and β and k are large (Giroud et al. 2000a).

It should be noted that:

$$j \frac{\sqrt{1+4\lambda}-1}{2} < \frac{\sqrt{1+4\lambda}-1}{2} < \frac{\sqrt{1+4\lambda+4\lambda^2}-1}{2} = \frac{(1+2\lambda)-1}{2} = \lambda \quad (6)$$

Therefore, regardless of the value of λ, Eq. 4 provides a conservative value of the maximum liquid thickness and a very good approximation for drainage layers involving geonets.

A parametric study of typical parameter values indicates that λ is rather small (i.e. less than 0.1) in all typical cases, except in the case of a liquid collection layer with a relatively low hydraulic conductivity (sand) placed on a slope that is not steep (e.g. less than 2%) and that is subjected to a high liquid impingement rate (e.g. above 0.1 m/day). Furthermore, in the case of geosynthetic liquid collection layers, λ is very small because the maximum liquid thickness is very small compared to the length of the liquid collection layer. Indeed, Eq. 14 shows that, if t_{max}/L is very small, λ is also very small. The shape of the liquid surface is then illustrated in Fig. 5c. The thickness at the top is zero and the maximum liquid thickness (which occurs at the toe) is small. Therefore, in the case of a geosynthetic liquid collection layer, the slope of the liquid surface is quasi parallel to the slope of the liquid collection layer and, as a result, the hydraulic gradient is equal to the classical value for flow parallel to a slope, $\sin\beta$. In contrast, in the case of a granular liquid collection layer, the slope of the liquid surface (Figs. 5a and 5b) increases from the top to the toe of the liquid collection layer. As a result, the hydraulic gradient increases from the top to the toe of the liquid collection layer, where it is significantly greater than $\sin\beta$.

4.3 Equivalency of geosynthetic to granular lateral drains

Regulatory equivalency between natural and geocomposite lateral drainage systems is currently based on equivalent transmissivity. However, Giroud et al. (2000c) have demonstrated that this practice is incorrect and non-conservative. An equivalency based solely on transmissivity will lead to selection of a geosynthetic drainage layer that may not provide adequate flow capacity and may result in the development of water pressure.

Equivalency between two lateral drainage systems must take into consideration the service flow gradients and maximum liquid thickness. Giroud et al. (2000c) have shown that, to be equivalent to a natural drainage layer, the minimum transmissivity of the geocomposite must be greater than the transmissivity of the natural drainage layer. The minimum transmissivity of the geonet is obtained by multiplying the transmissivity of the natural drainage layer by an equivalency factor, E. For natural drainage layers having maximum flow depths of 0.30 m, E can be approximated as follows:

$$E = \frac{1}{0.88}\left[1 + \frac{t_{prescribed}}{0.88\,L} \frac{\cos\beta}{\tan\beta}\right] \quad (7)$$

where $t_{prescribed}$ is the maximum liquid thickness prescribed by regulations. The equivalency defined by Eq. 7 is based on equal unconfined flow volumes in natural and geocomposite drainage systems. However, the very low heads associated with unconfined flow in a geocomposite lateral drain will result in a significantly reduced head acting on the underlying liner system, and therefore in a reduced potential leakage.

4.4 Double slopes

Two examples of liquid collection layers that comprise two sections with different slopes are

presented in Fig. 6 for a landfill cover system and a landfill leachate collection system. The two sections of a liquid collection layer are designated as the upstream section and the downstream section.
When a liquid collection layer comprises two sections, different liquid collection materials may be used in the two sections; for example, a geonet may be used on the steep slope and gravel may be used on the other slope. However, there are many applications where the same material is used in both sections; for example, a geonet may be used as the liquid collection layer in the various slopes of a landfill cover.

There are many cases, in particular in landfills, when a liquid collection layer comprises two sections with different slopes. If there is a drain between the two sections, each section can be treated as a liquid collection layer on a single slope, using the method presented by Giroud et al. (2000a). However, there are cases where there is no drain removing the liquid at the connection between the two sections. Those cases are addressed in Giroud et al. (2000b). They present a methodology to calculate the maximum thickness of liquid in each of the two sections of the liquid collection layer. The determination of the maximum thickness of liquid is an essential design step because the maximum liquid thickness must be less than an allowable thickness.

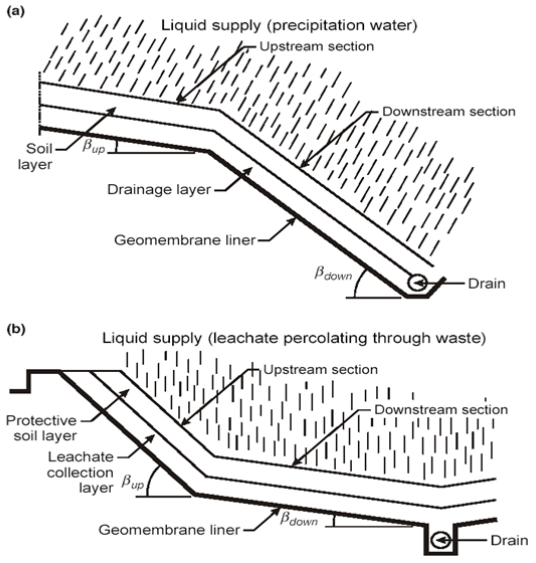

Figure 6. Liquid collection layers located on two different slopes: (a) drainage layer in landfill cover system; (b) leachate collection layer in a landfill (Giroud et al. 2000b).

The maximum liquid thickness in the downstream section of a two-slope liquid collection layer can be calculated using equations that account for both the *liquid impinging onto the downstream section* and the *liquid impinging onto*, and *flowing from*, the *upstream section*. The maximum liquid thickness in the upstream section of a two-slope liquid collection layer can be calculated using equations that depend on the material used in the upstream section and in the downstream section. In some cases, a transition zone is needed between the upstream and downstream sections.

5 REINFORCED COVER SYSTEMS

5.1 General considerations

The design of veneer slopes (e.g. steep cover systems for waste containment facilities) poses significant challenges to designers. The use of uniaxial reinforcements placed along the slope (under the veneer and above a typically strong mass of soil or solid waste) and anchored on the top of the slope has been a common design approach. However, this alternative may not be feasible for steep, long veneer slopes. As the veneer slope rests on top of a comparatively stronger mass solid waste, alternative approaches can be considered. This includes use of uniaxial reinforcements placed horizontally (rather than along the slope) and anchored into the underlying mass. A second alternative includes the use of fiber-reinforced soil. A review of analyses for veneers reinforced using horizontally placed inclusions is presented in this section.

This section presents an analytical framework for quantification of the reinforcement requirements for reinforced veneers where reinforcements are placed horizontally and embedded into a comparatively strong underlying mass. Emphasis in this evaluation is placed on the assessment of an infinite slope configuration. This allows direct comparison of the different reinforcement alternatives.

Design criteria for reinforced soil structure have been the focus of significant debate (Zornberg & Leshchinsky 2001). Although different definitions for the factor of safety have been reported for the design of reinforced soil slopes, the definition used in this study is relative to the shear strength of the soil:

$$FS = \frac{Available\ soil\ shear\ strength}{Soil\ shear\ stress\ required\ for\ equilibrium} \quad (8)$$

This definition is consistent with conventional limit equilibrium analysis, for which extensive experience has evolved for the analysis of unreinforced slopes. Current design practices for reinforced soil slopes often consider approaches that decouple the soil reinforcement interaction and do not strictly consider the factor of safety defined by Eq. 8. Such analyses neglect the influence of reinforcement forces on the soil stresses along the potential failure surface and may result in factors of safety significantly different than those calculated using more rigorous approaches. Considering the normal and shear forces acting in a control volume along the veneer slope (or infinite slope), and assuming a Mohr-Coulomb shear strength envelope, Eq. 8 can be expressed as:

$$FS = \frac{c + (N/L)\tan\phi}{S/L} \quad (9)$$

where N = normal force acting on the control volume; S = shear force acting on the control volume; L = length of the control volume; c = soil cohesion; and ϕ = soil friction angle.

Equations 8 and 9 are valid for both unreinforced and reinforced systems. In the case of an unreinforced veneer (Fig. 7), the shear and normal forces required for equilibrium of a control volume can be defined as a function of the weight of this control volume. That is:

$$S = W \sin\beta \quad (10)$$

$$N = W \cos\beta \quad (11)$$

$$W = \gamma L T \quad (12)$$

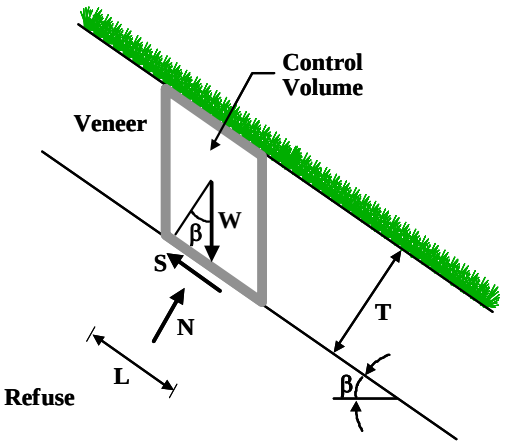

Figure 7. Unreinforced veneer

where W = weight of the control volume; β = slope inclination; T = veneer thickness; and γ = soil total unit weight.

From the previous equations, the classic expression for the factor of safety FS_u of an unreinforced veneer can be obtained:

$$FS_u = \frac{c}{\gamma T \sin\beta} + \frac{\tan\phi}{\tan\beta} \quad (13)$$

5.2 Covers reinforced with uniaxial geosynthetics parallel to the slope

Fig.8 shows a schematic representation of a cover system reinforced using uniaxial geosynthetics placed parallel to the slope. An infinite slope case is considered. In the case, the shear force needed for equilibrium of the control volume is smaller than the one in the unreinforced case. In this case, the shear force is defined by:

$$S = W \sin\beta - t_p L \quad (14)$$

where t_p = distributed reinforcement tensile stress of the reinforcement parallel to the slope. When the geosynthetic reinforcements are placed parallel to the slope, the distributed reinforcement tensile stress is a function of the allowable reinforcement tensile strength (T_a) and the total slope length (L_T), as follows:

$$t_p = \frac{T_a}{L_T} \quad (15)$$

From Equations 9, 14, 11, 12 and 15, the factor of safety for the parallel-reinforcement case, $FS_{r,p}$, can

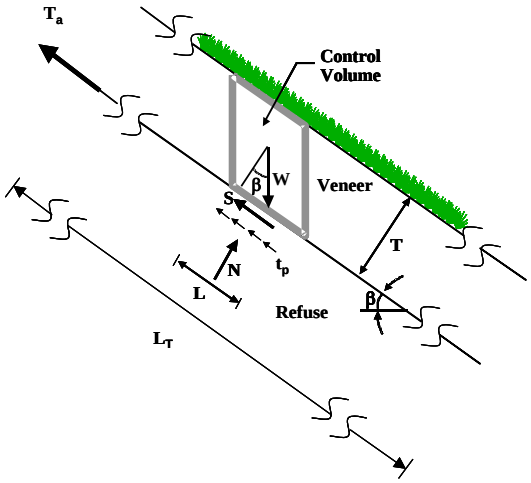

Figure 8. Veneer reinforced with uniaxial geosynthetic parallel to the slope

be estimated as:

$$FS_{r,p} = \frac{\frac{c}{\gamma\, T \sin\beta} + \frac{\tan\phi}{\tan\beta}}{1 - \frac{t_p}{\gamma\, T \sin\beta}} \qquad (16)$$

The eq. above can be simplified by defining the normalized distributed reinforcement tensile stress t_p^* (dimensionless), as follows:

$$t_p^* = \frac{t_p}{\gamma\, T} \qquad (17)$$

Using Eqs. 22 and 26 into Eq. 25:

$$FS_{r,p} = \frac{FS_u}{1 - t_p^* \frac{1}{\sin\beta}} \qquad (18)$$

Eq. 18 provides a convenient expression for stability evaluation of reinforced veneer slopes. It should be noted that if the distributed reinforcement tensile stress t equals zero (i.e. in the case of unreinforced veneers), Eq. 18 leads to $FS_{r,p} = FS_u$.

Even though the focus in this paper is on infinite slope analysis, typical design is performed using two-wedge finite slope analysis. Fig. 9 shows the geometry considered in the methodologies proposed by Giroud et al. (1995) and Koerner & Soong (1998). Some differences between these approaches in the adopted geometry are shown in the figure. More importantly, these approaches differ in the definition of the factor of safety.

Giroud et al. (1995a) do not include a factor of safety at the horizontal failure surface (AB) and define the factor of safety as the ratio between the resisting and the driving forces acting on the active wedge as projected on the slope direction. The factor of safety in this solution is the sum of five separate terms, which facilitates identification of the different contributions to the stability of the slope. Giroud et al (1995b) discuss stability analysis of veneer systems considering seepage forces. The analysis presented by Koerner & Soong (1998) is consistent with the generic definition of factor of safety stated by Eq. 8. Using the proposed method, the factor of safety is obtained by solving a quadratic equation. Koerner & Soong (1998) also provide analytical framework to address cases involving construction equipment, seepage forces, seismic forces, and the stabilizing effects of toe berms, tapered slopes and slope reinforcements. Thiel & Stewart (1993) and Punyamurthula & Hawk (1998) provide additional information regarding stability analysis of steep cover systems.

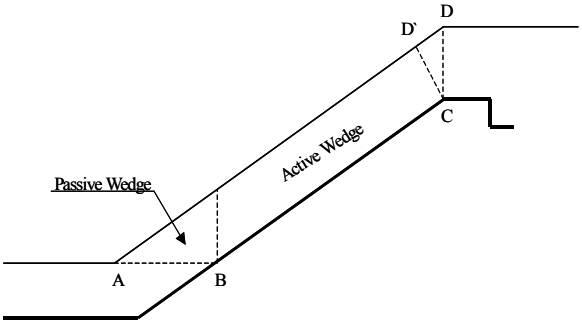

Figure 9: Schematic representation of the geometry of a cover for two-wedge finite slope analysis
Notes:
- ABC = slip surface
- CD = top of the cover soil as defined in the analysis by Koerner and Soong (1998)
- CD` = top of the cover soil as defined in the analysis by Giroud et al. (1995a)

5.3 Covers reinforced with horizontal uniaxial geosynthetics

Fig. 10 illustrates a cover (veneer) reinforced using horizontal uniaxial geosynthetics. Also in this case, the shear and normal forces acting on the control volume are defined not only as a function of the weight of the control volume, but also as a function of the tensile forces that develop within the reinforcements. For the purpose of the analyses presented herein, the reinforcement tensile forces are represented by a distributed reinforcement tensile stress t_h, which corresponds to a uniformly distributed tensile force per unit height. For a given slope with layers of reinforcement t_h can be expressed by:

$$t_h = \frac{T_a}{s} \qquad (19)$$

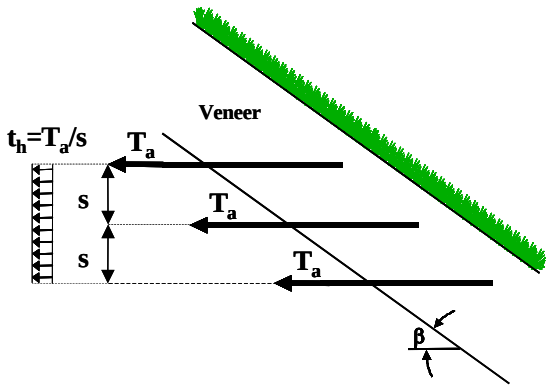

Figure 10. Veneer reinforced with horizontal uniaxial geosynthetics

where T_a = allowable reinforcement tensile strength and s = vertical spacing.

In this case, the shear and normal forces needed for equilibrium of a control volume are defined by:

$$S = W \sin\beta - t_h \; L \sin\beta\cos\beta \tag{20}$$

$$N = W \cos\beta + t_h \; L \sin^2\beta \tag{21}$$

From the previous equations, the following expression can be obtained for the factor of safety $FS_{r,h}$ of a veneer reinforced with horizontal uniaxial geosynthetics:

$$FS_{r,h} = \frac{\dfrac{c}{\gamma\, T \sin\beta} + \dfrac{\tan\phi}{\tan\beta} + \dfrac{t_h}{\gamma\, T}\sin\beta\tan\phi}{1 - \dfrac{t_h}{\gamma\, T}\cos\beta} \tag{22}$$

The eq. above can be simplified by defining the normalized distributed reinforcement tensile stress t_h* (dimensionless), as follows:

$$t_h^* = \frac{t_h}{\gamma\, T}\cos\beta \tag{23}$$

Using Eqs. 22 and 32 into Eq. 31 leads to:

$$FS_{r,h} = \frac{FS_u + t_h^* \tan\beta\tan\phi}{1 - t_h^*} \tag{24}$$

Eq. 24 provides a convenient expression for stability evaluation of reinforced veneer slopes. It should be noted that if the distributed reinforcement tensile stress t_h equals zero (i.e. in the case of unreinforced veneers), Eq. 24 leads to $FS_r = FS_u$

Additional aspects that should be accounted for in the design of reinforced veneer slopes include the evaluation of the pullout resistance (i.e. embedment length into the underlying mass), assessment of the factor of safety for surfaces that get partially into the underlying mass, evaluation of reinforcement vertical spacing, and analysis of seismic stability of the reinforced veneer.

5.4 Covers reinforced with randomly distributed fibers

A promising potential alternative for stabilization of steep landfill covers involves the use of fiber-reinforcement. Advantages of fiber-reinforcement over planar reinforcement in the stabilization of landfill covers are:

- Fiber-reinforcement is particularly suitable for stabilization of veneer slopes, as it provides additional shear strength under low confining pressures. A small increase of shear strength under low confinement has a significant impact on the stability of shallow slopes.
- Randomly distributed fibers helps maintaining strength isotropy and do not induce potential planes of weakness that can develop when using planar reinforcement elements.
- No anchorage is needed into solid waste as in the case of reinforcement with horizontal geosynthetics or at the crest of the slope as in the case of reinforcement parallel to the landfill slope.
- In addition to stabilizing the cover slopes, fiber reinforcement has the potential of mitigating the potential for crack development, providing erosion control, and facilitating the establishment of vegetation.

Relevant contributions have been made towards the understanding of the behavior of fibers. A soil mass reinforced with discrete, randomly distributed fibers is similar to a traditional reinforced soil system in its engineering properties but mimics admixture stabilization in the method of its preparation (Gray & Al-Refeai 1986; Bouazza & Amokrane 1995). Potential advantages of fiber-reinforced solutions over the use of other slope stabilization technologies have been identified, for example, for slope repairs in transportation infrastructure projects (Gregory & Chill 1998) and for the use of recycled and waste products such as shredded tires in soil reinforcement (Foose et al. 1996). Micro-reinforcement techniques

for soils also include the use of "Texol", which consists of monofilament fibers injected randomly into sand (Leflaive 1985) and the use of randomly distributed polymeric mesh elements (McGown et al. 1985; Morel & Gourc 1997). The use of fiber-reinforced clay backfill to mitigate the development of tension cracks was evaluated by several investigators (e.g. Al Wahab & El-Kedrah 1995). Several composite models have been proposed in the literature to explain the behavior of randomly distributed fibers within a soil mass. The proposed models have been based on mechanistic approaches (Maher & Gray 1990), on energy dissipation approaches (Michalowski & Zhao 1996), and on statistics-based approaches (Ranjar et al. 1996).

Fiber-reinforced soil has often been characterized as a single homogenized material, which has required laboratory characterization of composite fiber-reinforced soil specimen. The need for laboratory characterization has been a major drawback in the implementation of fiber-reinforcement in soil stabilization projects. To overcome this difficulty, a discrete approach that characterizes the fiber-reinforced soil as a two-component (fibers and soil) material was recently developed (Zornberg 2002). The main features of this approach are:

- The reinforced mass is characterized by the mechanical properties of individual fibers and of the soil matrix rather than by the mechanical properties of the fiber-reinforced composite material
- A critical confining pressure at which the governing mode of failure changes from fiber pullout to fiber breakage can be defined using the individual fiber and soil matrix properties.
- The fiber-induced distributed tension is a function of fiber content, fiber aspect ratio, and interface shear strength of individual fibers if the governing mode of failure is by fiber pullout.
- The fiber-induced distributed tension is a function of fiber content and ultimate tensile strength of individual fibers if the governing mode of failure is by fiber breakage.
- The discrete framework can be implemented into an infinite slope limit equilibrium framework. Convenient expressions can be obtained to estimate directly the required fiber content to achieve a target factor of safety.

The design methodology for fiber-reinforced soil structures using a discrete approach is consistent with current design guidelines for the use of continuous planar reinforcements and with the actual soil improvement mechanisms. Consequently, fiber-reinforced cover systems are expected to become an economical and technically superior alternative for reinforcement of landfill covers.

Fig. 11 shows a schematic view of a fiber-reinforced infinite slope. The behavior of the fiber-reinforced soil mass depends on whether the failure mode is governed by pullout or breakage of the fibers. The governing failure mode of the fiber-reinforced soil mass depends on the confinement. A critical normal stress, $\sigma_{n,crit}$, can be defined for comparison with the normal stress σ_n at the base of the veneer. If $\sigma_n < \sigma_{n,crit}$, the dominant mode of failure is the fibers pullout. This is the case for cover system applications. In this case, the fiber-induced distributed tension t_f is defined by (Zornberg 2002):

$$t_f = \eta \chi c_{i,c} \; c + \eta \chi c_{i,\phi} \tan\phi \, \sigma_n \qquad (25)$$

where $c_{i,c}$ and $c_{i,\phi}$ are the interaction coefficients for the cohesive and frictional components of the interface shear strength; η = aspect ratio (length/diameter) of the individual fibers, and χ = volumetric fiber content.

Similarly, if $\sigma_n > \sigma_{n,crit}$, the dominant mode of failure is fiber breakage. Even though this is not generally the governing mode of failure for cover slopes the solution for this case is presented for completeness. The fiber-induced distributed tension t_f is defined by:

$$t_t = \sigma_{f,ult} \cdot \chi \qquad (26)$$

where $\sigma_{f,ult}$ = ultimate tensile strength of the individual fiber.

In a fiber-reinforced veneer, the shear force needed for equilibrium of the control volume equals:

$$S = W \sin\beta - \alpha \, t_f \, L \qquad (27)$$

where α is an empirical coefficient that accounts for preferential orientation of fibers. For the case of randomly distributed fibers considered herein α equals one.

Using Eqs. 21, 22, and 20 into Eq. 34 leads to the factor of safety for a fiber-reinforced veneer, $FS_{r,f}$:

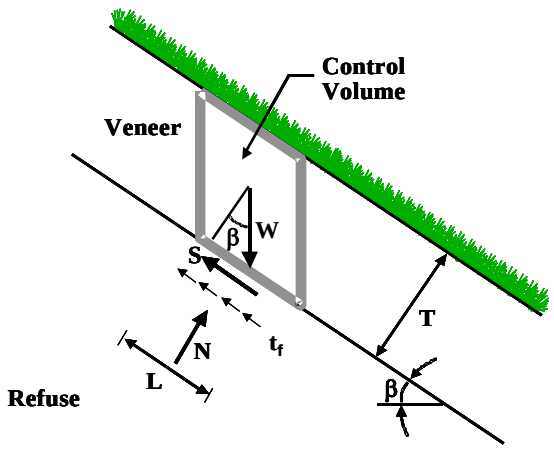

Figure 11. Veneer reinforced with randomly distributed fibers

$$FS_{r,f} = \frac{\dfrac{c}{\gamma\, T \sin\beta} + \dfrac{\tan\phi}{\tan\beta}}{1 - \dfrac{\alpha\, t_f}{\gamma\, T \sin\beta}} \qquad (28)$$

Defining the normalized distributed reinforcement tensile stress t_f^* (dimensionless) of a fiber-reinforced slope as follows:

$$t_f^* = \frac{t_f}{\gamma\, T} \qquad (29)$$

Consequently:

$$FS_{r,f} = \frac{FS_u}{1 - \alpha\, t_f^* \dfrac{1}{\sin\beta}} \qquad (30)$$

5.5 Comparison among different approaches for cover stability

The summary presented in this section provides a consistent framework for comparison of different reinforcement approaches for cover systems. They were all developed considering a consistent definition for the factor of safety (Eq. 8). Solutions are presented for the case of unreinforced, slope-parallel, horizontally-reinforced and fiber-reinforced veneers. Table 1 summarizes the expressions for the factor of safety in each case and the influence of the parameters governing the stability of the cover. As expected, additional reinforcement always leads to a higher factor of safety while increasing slope inclination would typically lead to decreasing stability. It is worth noting that increasing soil friction angle leads to increasing stability, when compared to the unreinforced case, only for the case of fiber reinforced slopes. It should also be noted that increasing total height of the slope (or increasing total length) does not affect detrimentally the efficiency of horizontally placed reinforcements and of fiber reinforcement.

The use of reinforced soil structures has also been extensively used for stabilization of waste cover systems. The design of these systems does not differ from the design of other applications such as transportation infrastructure. It should be noted, however, that the reinforced soil structures may be founded on highly compressible waste material. Additional projects involving use of reinforced soil structures to stabilize cover systems are presented by Cargill & Olen (1998).

Table 1. Effect of different terms in the factor of safety of cover systems

Definition of Factor of Safety				Influence on the factor of safety compared to FS_u			
				$t^* \nearrow$	$\beta \nearrow$	$\phi \nearrow$	L_T or H_T
Unreinforced veneer	$FS_u = \dfrac{c}{\gamma\, T \sin\beta} + \dfrac{\tan\phi}{\tan\beta}$						
Reinforcement parallel to slope	$FS_{r,p} = \dfrac{FS_u}{1 - t_p^* \dfrac{1}{\sin\beta}}$	with	$t_p^* = \dfrac{t_p}{\gamma\, T}$	↗	↘	↔	↘
Horizontal reinforcement	$FS_{r,h} = \dfrac{FS_u + t_h^* \sin\beta \tan\phi}{1 - t_h^* \cos\beta}$	with	$t_h^* = \dfrac{t_h}{\gamma\, T}$	↗	?	↗	↔
Fiber-reinforcement	$FS_{r,f} = \dfrac{FS_u}{1 - \alpha\, t_f^* \dfrac{1}{\sin\beta}}$	with	$t_f^* = \dfrac{t_f}{\gamma\, T}$	↗	↘	↗	↔

Notes:
t_p = distributed tensile stress per unit length of a cover with reinforcement parallel to the slope (Eq. 15)
t_h = distributed tensile stress per unit height of a cover with horizontal reinforcement (Eq. 19)
t_f = distributed tensile stress per unit length of a cover with fiber-reinforcement (Eq. 25)
Influence on FS: ↗ increasing; ↔ no influence; ↘ decreasing; ? either increasing or decreasing

5.6 Case histories

5.6.1 McColl Superfund site, Fullerton, California, US

This project is a good example of a site where multiple systems of soil reinforcement were used for stabilization of the final cover system. The soil reinforcement systems included the use of geogrid reinforcements, geocell systems, and reinforced buttress structures (Collins et al. 1998; Hendricker et al. 1998).

The site involves twelve pits containing petroleum sludges and oil-based drilling muds. The sludges were generated by the production of high-octane aviation fuel and were placed in the pits between 1942 and 1946. Between 1952 and 1964, the site was used for disposal of oil-based drilling muds. These wastes and their reaction products and by-products are found as liquid, gas and solid phases within the pits. At the time of deposition, essentially all of the waste materials were mobile. Over time, much of the waste had hardened. The drilling muds are a thixotropic semi-solid sludge, which can behave as a very viscous fluid.

Key considerations for the selection of the final remedy were to: (i) provide a cover system that includes a barrier layer and a gas collection and treatment system over the pits to minimize infiltration of water and release of hazardous or malodorous gas emissions; (ii) provide a subsurface vertical barrier around the pits to minimize outward lateral migration of mobile waste or waste by-products and inward lateral migration of subsurface liquid; and (iii) provide slope stability improvements for unstable slopes at the site.

The geogrid reinforcement for the cover system over the more stable pits was constructed with two layers of uniaxial reinforcement placed orthogonal to one another. Connections at the end of each geogrid roll were provided by Bodkin joints. Adjacent geogrid panels did not have any permanent mechanical connections. This was found to be somewhat problematic, as additional care was required during placement of the overlying gas collection sand to minimize geogrid separation. After the connections were made, the geogrid was covered with sand and then pull taut using a backhoe to pull on the end of the geogrid. Details of the cover system involving geogrid reinforcement are shown in Fig. 12.

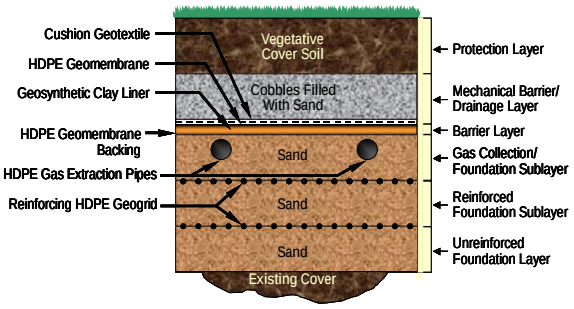

Figure 12. Cover system reinforced using uniaxial geogrids

A geocell reinforcement layer was constructed over the pits containing high percentages of drilling muds. While the construction of this reinforcement layer proceeded at a slower pace than the geogrid reinforcement, it did provide an immediate platform to support load. As the bearing capacity of the underlying drilling mud was quite low, the geocell provided load distribution, increasing the overall bearing capacity of the cover system. Details of the cover system involving geogrid reinforcement are shown in Fig. 13.

A total of three reinforced earth structures were constructed at the site. One of the structures was necessary to provide a working pad of reconstruction of the subsurface vertical barrier. This reinforced earth structure had to support the excavator with a gross operating weight of 1,100 kN that was used to dig the soil-bentonite cutoff wall. Another reinforced earth structure at the site had to span a portion of completed cutoff wall. Due to concerns that the stress of the reinforced earth structure on the underlying soil-bentonite cutoff wall would lead to excessive deformation of the wall due to consolidation of the cutoff wall backfill, a flexible wall fascia was selected. As shown in Fig. 14, a soldier pile wall was constructed to provide stability of the system during construction. The use of

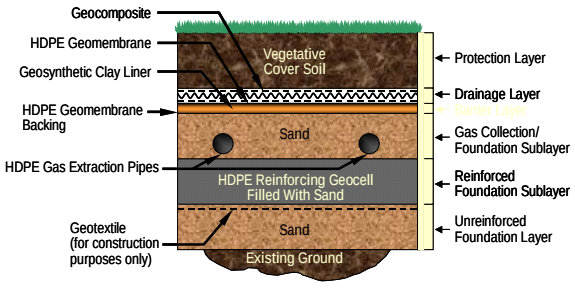

Figure 13. Cover system reinforced using geocells

geosynthetic alternatives in this project was more suitable and cost effective than their conventional counterparts.

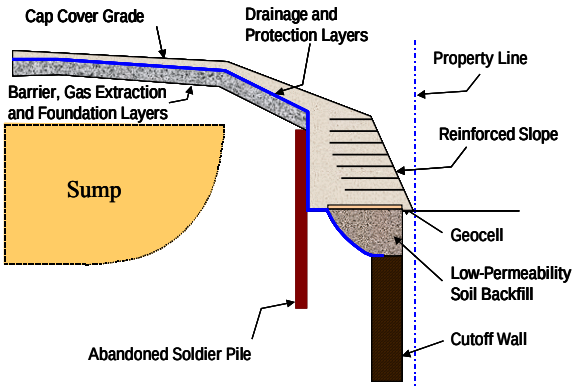

Figure 14. Buttressing reinforced slope at McColl Superfund site

5.6.2 North Slopes at OII Superfund site, Monterey Park, California, US

A cover reinforced using horizontally placed geogrids was constructed as part of the final closure of the Operating Industries, Inc. (OII) landfill. This case history highlights the final closure of a hazardous waste landfill where the severe site constraints were overcome by designing and constructing an alternative final cover incorporating horizontal geosynthetic veneer reinforcement (Zornberg et al. 2001).

The 60-hectare south parcel of the OII landfill was operated from 1948 to 1984, receiving approximately 30-million cubic meters of municipal, industrial, liquid and hazardous wastes. In 1986, the landfill was placed on the National Priorities List of Superfund sites. Beginning in 1996, the design of a final cover system consisting of an alternative evapotranspirative soil cover was initiated, and subsequent construction was carried out from 1997 to 2000. The refuse prism, which occupies an area of about 50 hectares, rises approximately 35 m to 65 m above the surrounding terrain. Slopes of varying steepness surround a relatively flat top deck of about 15 hectares.

The final cover design criteria mandated by the U.S. Environmental Protection Agency (EPA) had to satisfy criteria for percolation performance, static and seismic stability of the steep sideslopes of the landfill, and erosion control. Stability criteria required a static factor of safety of 1.5, and acceptable permanent seismically induced deformations less than 150 mm under the maximum credible earthquake. The basis of the seismic stability criteria is that some limited deformation or damage may result from the design earthquake, and that interim and permanent repairs would be implemented within a defined period.

One of the most challenging design and construction features of the project was related to the north slope of the landfill. The north slope is located immediately adjacent to the heavily travelled Pomona freeway (over a distance of about 1400 meters), rises up to 65 meters above the freeway, and consists of slope segments as steep as 1.5:1 (H:V) and up to 30 m high separated by narrow benches. The toe of the North Slope and the edge of refuse extends up to the freeway. The pre-existing cover on the North Slope consisted of varying thickness (a few centimetres to several meters) of non-engineered fill. The cover included several areas of sloughing instability, chronic cracking and high level of gas emissions. The slope was too steep to accommodate a layered final cover system, particularly a cover incorporating geosynthetic components (geomembranes or GCL). Because of the height of the slope and lack of space at the toe, it was not feasible to flatten the slope by pushing out the toe, removing refuse at the top, or constructing a retaining / buttress structure at the toe of slope.

After evaluating various alternatives, an evapotranspirative cover incorporating geogrid reinforcement for veneer stability was selected as the appropriate cover for the North Slope. The evapotranspirative cover had additional advantages over traditional layered cover systems, including superior long-term percolation performance in arid climates, ability to accommodate long-term settlements, good constructability, and ease of long-term operations and maintenance. The selected cover system included the following components, from the top down: 1) vegetation to promote evapotranspiration and provide erosion protection; 2) a 1.2 m – thick evapotranspirative soil layer to provide moisture retention, minimize downward migration of moisture, and provide a viable zone for root growth; and 3) a foundation layer consisting of soil and refuse of variable thickness to provide a firm foundation for the soil cover system.

Stability analyses showed that for most available evapotranspirative materials, compacted to practically achievable levels of relative compaction on a 1.5:1 slope (e.g. 95% of Standard Proctor), the minimum static and seismic stability criteria were not met. Veneer geogrid reinforcement with horizontally placed geogrids was then selected as the most appropriate and cost-effective method for stabilizing the North Slope cover. The analytical framework was used in the design. Fig. 15 shows the typical veneer reinforcement detail selected based on the shear strength of the soils used in construction.
The veneer reinforcement consisted of polypropylene uniaxial geogrids, installed at 1.5-m vertical intervals for slopes steeper than 1.8:1, and at 3-m vertical intervals for slopes between 2:1 and 1.8:1. The geogrid panels are embedded a minimum of 0.75 m into the exposed refuse slope face from which the pre-existing cover had been stripped. The geogrid panels were curtailed approximately 0.3 to 0.6 m away from the finished surface of the slope cover. This was done to permit surface construction, operation and maintenance activities on the slope face without the risk of exposing or snagging the geogrid.

Construction of the North Slope was accomplished in 12 months. Approximately 500,000 m^3 of soil and 170,000 m^2 of geogrid were placed. Total area of geogrid placement exceeded 9.3 hectares. The maximum height of reinforced portion of the landfill slopes was 55 m (the maximum height of the total landfill slope was 65 m).

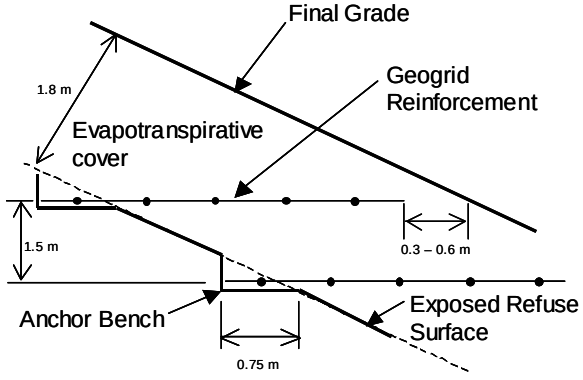

Figure 15. Reinforcement detail for horizontal reinforcement anchored into solid waste (from Zornberg et al. 2001)

5.6.3 Toe Buttress at OII Superfund site, Monterey Park, California, US

In addition to the project described in Case 6, a geogrid-reinforced toe buttress was constructed in 1987 at the OII Superfund site in order to enhance the stability of the southeastern slopes of the OII Landfill Superfund site (Zornberg and Kavazanjian, 2001). The toe buttress is immediately adjacent to a residential development. The waste slopes behind the toe buttress are up to 37 m high with intermediate slopes between benches up to 18 m high and as steep as 1.3H:1V.

The approximately 4.6 m high, 460 m long toe buttress was built using sandy gravel as backfill material. The front of the structure was founded on concrete piers. However, as the back of the toe buttress was founded on waste, the structure has been subjected to more than 0.6 m of differential settlements since the end of its construction. In response to concerns regarding the internal stability of the reinforced soil structure, finite element analyses were performed to evaluate the long-term integrity of the geogrid reinforcements under static and seismic loads. The analyses considered 40 years of settlement followed by the design earthquake. The finite element modeling evaluated the strains induced in the geogrid reinforcement considering both material and geometric nonlinearity. The analyses were performed in three sequential phases: (i) toe buttress construction, modeled by sequentially activating soil and bar elements in the reinforced soil zone; (ii) gradual increase in differential settlements, simulated by imposing incremental displacements at the base of the reinforced soil mass; and (iii) earthquake loading, modeled by applying horizontal body forces representing the maximum average acceleration estimated in a finite element site response analysis.

A total of 2.0 m of differential settlement was imposed on the base of the finite element mesh to simulate long-term differential settlement. The maximum strain in the geogrid reinforcements calculated after this long-term static loading was less than 3.0 percent, well below the allowable static strain of 10 percent. The calculated maximum geogrid strain induced by construction, long-term differential settlement, and earthquake loading was approximately 8.5 percent, well below the allowable strain of 20 percent established for rapid loading. The results of this study indicate that the integrity of the geogrid-reinforced toe buttress should be

maintained even when subjected to large differential settlements and severe earthquake loads.

6 EXPOSED GEOMEMBRANE COVER SYSTEMS

Exposed geomembrane covers have been recently analyzed, designed, and constructed to provide temporary and final closure to waste containment facilities. Significant cost savings may result from elimination of topsoil, cover soil, drainage, and vegetation components in typical cover systems. Additional advantages include reduced annual operation and maintenance requirements, increased landfill volume, easier access to landfilled materials for future reclamation, and reduced post-construction settlements. In addition, if the landfill slopes are steep, the use of exposed geomembrane covers may provide solution to erosion concerns and to stability problems associated with comparatively low interface shear strength of typical cover components. Disadvantages associated with the use of exposed geomembrane covers include increased vulnerability to environmental damage, increased volume and velocity of stormwater runoff, limited regulatory approval, and aesthetics concerns. However, exposed geomembrane covers have been particularly applicable to sites where the design life of the cover is relatively short, when future removal of the cover system may be required, when the landfill sideslopes are steep, when cover soil materials are prohibitively expensive, or when the landfill is expected to be expanded vertically in the future. In particular, the current trend towards the use of "leachate recirculation" or bioreactor landfills makes the use of exposed geomembrane covers a good choice during the period of accelerated settlement of the waste. Key aspects in the design of exposed geomembrane covers are assessment of the geomembrane stresses induced by wind uplift and of the anchorage against wind action (Giroud et al. 1995; Zornberg & Giroud1997; Gleason et al. 2001).

6.1 Geomembrane stresses induced by wind uplift

The resistance to wind uplift of an exposed geomembrane cover is a governing factor in its design. Wind uplift of the geomembrane is a function of the mechanical properties of the geomembrane, the landfill slope geometry, and the design wind velocity. Procedures for the analysis of geomembrane wind uplift have been developed by Giroud et al. (1995) and Zornberg & Giroud (1997). Additional guidelines are provided by Wayne & Koerner (1988). A number of exposed geomembrane covers have been designed and constructed using these procedures (Gleason et al. 2001).

Wind uplift design considerations involve assessment of the maximum wind velocity that an exposed geomembrane can withstand without being uplifted, of the required thickness of a protective layer that would prevent the geomembrane from being uplifted, of the tension and strain induced in the geomembrane by wind loads, and of the geometry of the uplifted geomembrane. The fundamental relationship of the geomembrane uplift problem is the "uplift tension-strain relationship" defined by (Zornberg & Giroud 1997):

$$\varepsilon_w = \frac{2T}{S_e L} \sin^{-1}\left[\frac{S_e L}{2T}\right] - 1 \qquad (31)$$

where: ε_w = geomembrane strain component induced by wind uplift; T = total geomembrane tension; S_e = effective wind-induced suction; and L = length of geomembrane subjected to suction. Fig. 16 shows a schematic representation of an uplifted geomembrane. It should be noted that the uplift tension-strain relationship (Eq. 31) relates the strain induced only by the wind (ε_w) with the total tension in the geomembrane (T) induced also by other sources like temperature or gravity. In other words, Eq. 31 is not a relationship between the wind-induced strain (ε_w) and the wind-induced tension (T_w).

The wind uplift pressure, S_e can be estimated for a given wind velocity as (Giroud et al.1995):

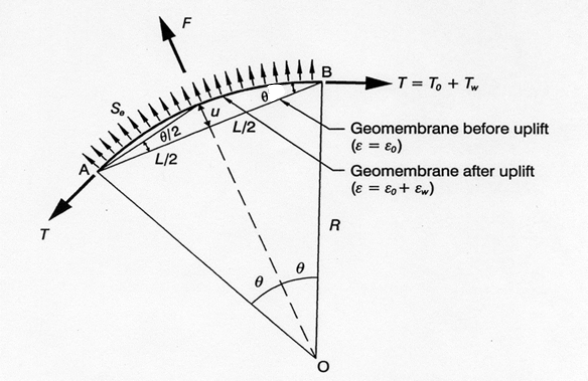

Figure 16. Uplifted geomembrane (Zornberg & Giroud 1997)

$$S_e = 0.6465\,V^2 \qquad (32)$$

Two solutions are available for tension in a geomembrane due to wind uplift: one for the simple condition of a linear stiffness for the geomembrane, and a second solution for a nonlinear stiffness. If the geomembrane tension-strain curve, or a portion of it, can be assumed to be linear, ε_w can be estimated using the geomembrane tensile stiffness J, the initial tension T_0, the effective suction S_e , and the geomembrane length L by solving the following eq. (Zornberg and Giroud1997):

$$\frac{S_e L}{2(T_0 + J\varepsilon_w)} = \sin\left[\frac{S_e L}{2(T_0 + J\varepsilon_w)}(1+\varepsilon_w)\right] \qquad (33)$$

The expression above may be solved by trial and error in order to determine ε_w. After determining the wind-induced strain component, ε_w, the tension component induced by wind, T_w , can also be estimated using the geomembrane tensile stiffness J .

6.2 Anchorage against wind action

Alternative means have been proposed to provide anchorage to the exposed geomembrane cover to resist uplift forces. A method for designing anchor benches and trenches used to secure geomembranes exposed to wind action was presented by Giroud et al. (1999). Fig. 17 shows a typical anchor bench. Three potential failure mechanisms are identified: (i) sliding of the anchor bench or trench in the downslope direction; (ii) sliding of the anchor bench or trench in the upslope direction; and (iii) uplifting of the anchor bench or trench. It is shown that the first mechanism is the most likely and that the third mechanism is the least likely. Criteria are provided by Giroud et al. (1999) to determine the potential failure mechanism in each specific situation. This is defined by the geometry of the slope on which the geomembrane is resting and the geomembrane tensions induced by wind action. It is also shown that a simple method, consisting of only checking the resistance of anchor benches and trenches against uplifting is unconservative as lateral sliding is more likely to occur than uplifting.

6.3 Case histories

A number of exposed geomembrane covers have been recently designed using the aforementioned procedures for wind uplift analysis. Four of the recently constructed exposed geomembrane covers in the US are listed below (Gleason et al. 1998,

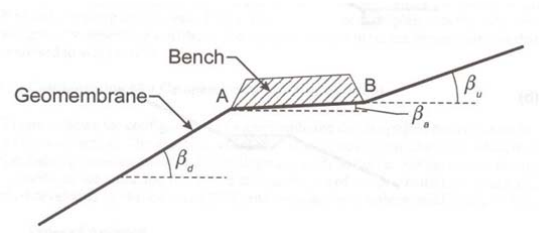

Figure 17. Configuration of an anchor bench to prevent wind uplift in an exposed geomembrane cover (Giroud et al. 1999)

Gleason et al. 2001; Zornberg et al. 1997). A fifth case history is detailed next. At each landfill, the design and operations criteria for the exposed geomembrane cover, as well as the rationale for constructing the exposed geomembrane cover were significantly different. The sites are:

- Crossroads Landfill, Norridgewock, Maine: an exposed geomembrane cover was designed and installed over a 2-ha landfill that had reached its allowable interim grades based on site subsurface stability. With time, the subsurface strata of clay beneath the landfill will consolidate and gain shear strength, thus allowing for additional waste placement.
- Naples Landfill, Naples, Florida: an exposed geomembrane cover was designed to provide a temporary cover for a 9-ha landfill for two purposes: (i) the exposed geomembrane cover was constructed a year prior to the planned construction of a typical final cover system in order to control odors associated with landfill gas; and (ii) on two of these slopes, the exposed geomembrane cover was installed over areas that will be overfilled in the near future.
- Sabine Parish Landfill, Many, Louisiana: an exposed geomembrane cover was designed and installed over a 6-ha landfill that had severe erosion because of long steep sideslopes that could not be reasonably closed using conventional closure system technology.
- A feasibility evaluation of the use of an exposed geomembrane cover was conducted for the OII Superfund landfill. The main reason for having considered an exposed geomembrane cover at this site was the difficulty in demonstrating adequate slope stability, under static and seismic conditions, in the case of conventional covers where geosynthetics are overlain by soil layers. Although an evapotranspirative cover system

was finally adopted at the site, an exposed geomembrane cover was also considered because it would have been stable under both static and seismic conditions.

6.3.1 *Delaware Solid Waste Authority (DSWA), Sussex County, Delaware, US*

An exposed geomembrane cover was designed and installed over a 17-ha landfill to provide a long-term cover system (i.e. 10 to 20 years) over waste that may be reclaimed at a later date (Gleason et al. 1998). Several geomembranes were considered for the design of the exposed cover system. Calculations for the selected geomembrane involved determination of resistance to wind uplift. A reinforced geomembrane with a linear stress-strain curve characterized by a tensile stiffness, J = 165 kN/m and a strain at break of 27% was selected for the design. The geomembrane anchors on the cover system were designed to include a swale that conveys storm-water runoff from the landfill in a non-erosive manner.

Fig. 18 shows the exposed geomembrane cover placed over Cells 1 and 2 at the DSWA's southern facility. This cover was placed over 5% to 4H:1V slopes. The exposed geomembrane cover will be removed to allow potential mining of the in-place waste and placement of additional waste into the cells. A 0.9 mm green polypropylene geomembrane with a polyester scrim reinforced was used. In this application, the interface friction required of the geomembrane is defined by the swale anchorage structure.

Figure 18. Exposed geomembrane cover over Cells 1 and 2 of the DSWA's southern facility.

7 CONCLUSIONS

This paper focuses on recent advances in the use of geosynthetics in environmental applications. When designing GCL-lined slopes it is essential to recognize the differences in interface and internal shear strengths. Significant have been recently compiled, which provide good understanding of the probabilistic distributions of the peak and large displacement strength values. These results are suitable for future reliability based stability analyses. Calculating the thickness of liquid in a liquid collection layer is an important design step because one of the design criteria for a liquid collection layer is that the maximum thickness of the liquid collection layer must be less than an allowable thickness. Simple equations have been developed to calculate the maximum thickness of liquid in a liquid collection layer. Such equations are suitable to define transmissivity requirements of liquid collection layers in single and double slopes.

Major advances have recently taken place regarding the use of geosynthetic reinforcements to allow significantly steep and high final cover systems. Solutions are presented for the case of unreinforced, slope-parallel, horizontally-reinforced and fiber-reinforced veneers. As expected, additional reinforcement always leads to a higher factor of safety while increasing slope inclination would typically lead to decreasing stability. Increasing soil friction angle leads to significant increase in stability, when compared to the unreinforced case, only for the case of fiber reinforced slopes. Increasing total height of the slope (or increasing total length) does not affect detrimentally the efficiency of horizontally placed reinforcements and of fiber reinforcement.

Exposed geomembrane covers have been recently analyzed, designed, and constructed to provide temporary and final closure to waste containment facilities. Key aspects in the design of exposed geomembrane covers are assessment of the geomembrane stresses induced by wind uplift and of the anchorage against wind action. Procedures for the analysis of geomembrane wind uplift and methods for designing anchor benches and trenches used to secure geomembranes exposed to wind action have also been developed. The use of exposed geomembrane covers is particularly suitable in sites with steep landfill slopes and in landfills where leachate recirculation is considered.

8 REFERENCES

Al Wahab, R.M. & El-Kedrah, M.M. 1995. Using fibers to reduce tension cracks and shrink/swell in compacted clays. Geoenvironment 2000, ASCE Geot. Sp. Publication 46: 433-446.

Bouazza, M., Zornberg, J.G., and Adam, D. (2002). "Geosynthetics in Waste Containment Facilities: Recent Advances." Keynote paper, Proc. Seventh Intl. Conf. on Geosynthetics, Nice, France, 22-27 September, A.A. Balkema, Vol. 2, pp. 445-510.

Bouazza, A. & Amokrane, K. 1995. Granular soil reinforced with randomly distributed fibres. Proc. 11th African Regional Conf. on Soil Mech. & Foundation Eng., Cairo: 207-216.

Bressi, G., Zinessi, M., Montanelli, F. & Rimoldi, P. 1995. The slope stability of GCL layers in geosynthetic lining system. Proc. 5th Intl. Symp. on Landfills, Cagliari 1: 595-610.

Byrne, R.J., Kendall, J. & Brown, S. 1992. Cause and mechanism of failure, Kettleman hills landfill B-19, Unit 1A. Stability and Performance of Slopes and Embankments, ASCE. Geot. Sp. Publication 31: 1188-1520.

Cancelli, A. & Cazzuffi, D. 1994. Env. aspects of geosynthetic applications in landfills and dams. Proc. 5th Intl. Conf. on Geosynthetics, Singapore 4: 55-96.

Cargill, K.W. & Olen, K.L. 1998. Landfill closure using reinforced soil slopes. Proc. 6th Intl. Conf. on Geosynthetics, Atlanta : 481-486.

Cazzuffi, D., 1987. The use of geomembranes in Italian dams. Intl. J. of Water Power and Dam Construction 26(2): 44-52.

Collins, P., Ng, A.S. & Ramanujam, R. 1998. Superfund success, superfast. Civil Eng., Decembre: 42-45.

Daniel, D. E., Koerner, R., Bonaparte, R., Landreth, R., Carson, D. & Scranton, H. 1998. Slope stability of geosynthetic clay liner test plots. J. of Geot. and GeoEnv. Eng. 124(7): 628-637.

Eid, H.T & Stark, T.D. 1997. Shear behaviour of an unreinforced geosynthetic clay liner. Geosynthetics Intl. 4(6): 645-659.

Eid, H.T., Stark, T.D. & Doerfler, C.K. 1999. Effect of shear displacement rate on internal shear strength of a reinforced geosynthetic clay liners. Geosynthetics Intl. 6(3): 219-239.

Feki, N., Garcin, P., Faure, Y.H., Gourc, J.P. & Berroir, G. 1997. Shear strength tests on geosynthetic clay liner systems. Proc. Geosynthetics 97, Long Beach 2: 899-912.

Foose, G.J., Benson, C.H. & Bosscher, P.J. 1996. Sand reinforced with shredded waste tires. J. of Geot. Eng. 122 (9): 760-767.

Fox, P. J., Rowland, M.G. & Scheite, J.R. 1998a. Internal shear strength of three geosynthetic clay liners. J. of Geot. and GeoEnv. Eng. 124 (10): 933-944.

Frobel, R.K. 1996. Geosynthetic clay liners, part four: interface and internal shear strength determination. Geot. Fabric Report 14(8): 20-23.

Garcin, P., Faure, Y.H., Gourc, J.P. & Purwanto, E. 1995. Behaviour of geosynthetic clay liner (GCL): laboratory tests. Proc. 5th Intl. Symp. on Landfills, Cagliari (1): 347-358.

Gilbert, R.B., Fernandez, F. & Horsfield, D.W. 1996. Shear strength of reinforced GCLs. J. of Geot. Eng. 122 (4): 259-266.

Gilbert, R.B., Liu, C.N., Wright, S.G. & Trautwein, S.J. 1995. A double shear test method for measuring interface strength. Proc. Geosynthetics 95 Conf., Nashville 3: 1017-1029.

Giroud, J.P. & Cazzuffi, D.A. 1989. Uses of geosynthetics for Env. control. Proc. of 12th Intl. Conf. on Soil Mech. and Foundation Eng., Rio de Janeiro, Brazil (4): 3119-3125.

Giroud, J.P., Gleason, M.H. & Zornberg, J.G. 1999. Design of geomembrane anchorage against wind action. Geosynthetics Intl. 6(6): 481-507.

Giroud, J.P., Zornberg, J.G. & Zhao, A. 2000a. Hydraulic design of geosynthetic and granular liquid collection Layers. Geosynthetics Intl., Sp. Issue on Liquid Collection Systems 7(4-6): 285-380.

Giroud, J.P., Zornberg, J.G. & Beach, J.F. 2000b. Hydraulic design of geosynthetic and granular liquid collection layers comprising two different slopes. Geosynthetics Intl., Sp. Issue on Liquid Collection Systems 7(4-6): 453-489.

Giroud, J.P., Zhao, A. & Bonaparte, R. 2000c. The myth of hydraulic transmissivity equivalency between geosynthetic and granular liquid collection layers. Geosynthetics Intl., Sp. Issue on Liquid Collection Systems 7(4-6): 381-401.

Giroud, J.P., Pelte, T. & Bathurst, R.J., 1995. Uplift of geomembranes by wind. Geosynthetics Intl., 2(6): 897-952.

Giroud, J.P., Williams, N.D., Pelte, T. & Beech, J.F. 1995a. Stability of geosynthetic-soil layered systems on slopes. Geosynthetics Intl. 2(6): 1115-1148.

Giroud, J.P., Bachus, R.C. & Bonaparte R. 1995b. Influence of water flow on the stability of geosynthetic-soil layered systems on slopes. Geosynthetics Intl. 2(6): 1149-1180

Gleason, M.H., Houlihan, M.F. & Palutis, J.R. 2001. Exposed geomembrane cover systems: technology summary. Proc. Geosynthetics 2001 Conf., Portland: 905-918.

Gourc, J.P. 1994. Geosynthetics and environment Eng.. The Mercer Lecture. Proc. 13th Intl. Conf. on Soil Mech. and Foundation Eng., New Delhi (4): 65-86.

Gray, D.H. & Al-Refeai, T. 1986. Behaviour of fabric versus fiber-reinforced Sand. J. of Geot. Eng. 112(8): 804-820. Gregory, G. H. & Chill, D. S. 1998. Stabilization of earth slopes with fiber-reinforcement. Proc. 6th Intl. Conf. on Geosynthetics, IFAI, Atlanta (2): 1073-1078.

Hendricker, A.T., Fredianelli, K.H., Kavazanjian, E. & McKelvey, J.A. 1998. Reinforcement requirements at a hazardous waste site. Proc. 6th Intl. Conf. on Geosynthetics. IFAI, Atlanta (1): 465-468.

Koerner, R.M. 1990. Preservation of the environment via geosynthetic containment systems. Proc. of 4th Intl. Conf. on Geosynthetics, The Hague (3): 975-988.

Koerner, R.M. & Soong, T.Y. 1998. Analysis and design of veneer cover soils. Proc. 6th Intl. Conf. on Geosynthetics, Atlanta 1: 1-23

Leflaive, E. 1985. Soils reinforced with continuous yarns: the Texol. Proc. 11th Intl. Conf. On Soil Mech. and Foundation Eng., San Francisco 3: 1787-1790.

Maher, M.H. & Gray, D.H. 1990. Static response of sand reinforced with randomly distributed fibers. J. Geot. Eng. 116(1): 1661-1677.

Manassero, M., Parker, R., Pasqualini, E., Szabo, I., Almeida, M.S.S, Bouazza, A., Daniel, D.E & Rowe, R.K 1998. Controlled landfill design (Geot. aspects). Proc. 3rd Intl. Congress on Env. Geotechnics, Lisbon 3: 1001-1038.

McCartney, J.S., Zornberg, J.G. & Swan, R. 2002. Internal and Interface Shear Strength of Geosynthetic Clay Liners (GCLs). Geot. Research Report, Department of CEAE, U. of Colorado at Boulder, 386 pages.

McGown, A., Andrawes, K.Z, Hytiris, N. & Mercel, F.B. 1985. Soil strengthening using randomly distributed mesh elements. Proc. 11th Intl. Conf. On Soil Mech. and Foundation Eng., San Francisco 3: 1735-1738.

McEnroe, B.M. 1993. Maximum satureated depth ofver landfill liner. J. of Env. Eng. 119(2): 262-270.

Michalowski, R.L. & Zhao, A. 1996. Failure of fiber-reinforced granular soils. J. Geot. Eng. 122(3): 226-234.

Morel, J.C. & Gourc, J.P. 1997. Mechanical behavior of sand reinforced with mesh elements. Geosynthetics Intl. 4(5): 481-508.

Punyamurthula, S. & Hawk, D. 1998. Issues with Slope Stability of Landfill Cover Systems. Proc. 12th GRI Conf., Folsom: 259-268

Ranjan, G., Vassan, R.M. & Charan, H.D. 1996. Probabilistic Analysis of Randomly Distributed Fiber-Reinforced Soil. J. Geot. Eng. 120(6): 419-426.

Richardson, G.N. 1997. GCL internal shear strength requirements. Geotechnical Fabric Report 15(2): 20-25.

Rowe, R.K 1998. Geosynthetics and the minimization of contaminant migration through barrier systems beneath solid waste. Proc. 6th Intl. Conf. on Geosynthetics, Atlanta 1: 27-102.

Rowe, R.K., Quigley, R.M. & Booker, J.R. 1995. Clayey Barrier Systems for Waste Disposal Facilities, E & FN Spon (Chapman & Hall), London, 390 p.

Stark, T.D. & Eid, H.T. 1996. Shear behaviour of reinforced geosynthetic clay liners. Geosynthetics Intl. 3(6): 771-786.

Stark, T. D., Arellano, D., Evans, W.D., Wilson, V.L. & Gonda, J.M. 1998. Unreinforced geosynthetic clay liners case history. Geosynthetics Intl. 5(5): 521-544.

Tanays, E., Le Tellier, I., Bernhard, C. & Gourc, J.P. 1994. Behaviour of lining systems on waste landfill slopes: an experimental approach. Proc. 5th Intl. Conf. on Geotextiles, Geomembranes and Related Products, Singapore 3: 977-980.

Terzaghi, K. & Lacroix, Y. 1964. Mission Dam: an earth and rockfill dam on a highly compressible foundation. Geotechnique 14(1): 13-50.

Thiel, R.S. & Stewart, M.G. 1993. Geosynthetic landfill cover design methodology and construction experience in the pacific northwest. Proc. Geosynthetics 93 Conf., Vancouver: 1131-1144

Triplett, E.J. & Fox, P.J. 2001. Shear strength of HDPE geomembrane/geosynthetic clay liner interface. J. of Geot. & GeoEnv. Eng. 127(6): 543-552.

Von Maubeuge, K.P. & Eberle, M. 1998. Can geosynthetic clay liners be used on slopes to achieve long-term stability. Proc. 3rd Intl. Congress on Env. Geotechnics, Lisbon 1: 375-380

Wayne, M.H. & Koerner, R.M., 1998. Effect of wind uplift on liner systems. Geot. Fabrics Report, July/August.

Zornberg, J.G. (2002). “Discrete Framework for Limit Equilibrium Analysis of Fibre-Reinforced Soil.” Géotechnique, Vol. 52, No. 8, pp. 593-604.

Zornberg, J.G. & Christopher, B.R. 2007. Geosynthetics. Chapter 37, The Handbook of Groundwater Eng., Jacques W. Delleur (Editor-in-Chief), CRC Press, Inc., Boca Raton, Florida.

Zornberg, J.G. & Giroud, J.P. 1997. Uplift of geomembranes by wind - extension of equations. Geosynthetics Intl. 4(2): 187-207.

Zornberg, J.G. & Kavazanjian, E. 2001. Prediction of the performance of a geogrid-reinforced slope founded on solid waste. Soils and Found. 41(6): 1-16.

Zornberg, J.G. & Leshchinsky, D. 2001. Comparison of Intl. Design Criteria for Geosynthetic-Reinforced Soil Structures. Geosynthetics and Earth Reinforcement, H. Ochiai, J. Otani, and Y. Miyata (Editors), ISSMGE-TC9 report: 106-117.

Zornberg, J.G., Somasundaram, S. & LaFountain, L. 2001. Design of Geosynthetic-Reinforced Veneer Slopes. Proc. Intl. Symp. on Earth Reinforcement: Landmarks in Earth Reinforcement, Fukuoka: 305-310.